

# Excitation hierarchy of the quantum sine-Gordon spin chain in strong magnetic field

S. A. Zvyagin,<sup>1</sup> A. K. Kolezhuk,<sup>2,3</sup> J. Krzystek,<sup>1</sup> and R. Feyerherm<sup>4</sup>

<sup>1</sup>*National High Magnetic Field Laboratory, Florida State University, Tallahassee, FL 32310*

<sup>2</sup>*Institute of Magnetism, National Academy of Sciences, 03142 Kiev, Ukraine*

<sup>3</sup>*Institut für Theoretische Physik, Universität Hannover, 30167 Hannover, Germany*

<sup>4</sup>*Hahn-Meitner-Institute (HMI), 14109 Berlin, Germany*

The magnetic excitation spectrum of copper pyrimidine dinitrate, a material containing  $S = \frac{1}{2}$  antiferromagnetic chains with alternating  $g$ -tensor and the Dzyaloshinskii-Moriya interaction, and exhibiting a field-induced spin gap, is probed using submillimeter wave electron spin resonance spectroscopy. Ten excitation modes are resolved in the low-temperature spectrum, and their frequency-field diagram is systematically studied in magnetic fields up to 25 T. The experimental data are sufficiently detailed to make a very accurate comparison with predictions based on the quantum sine-Gordon field theory. Signatures of three breather branches and a soliton, as well as those of several multi-particle excitation modes are identified.

PACS numbers: 75.40.Gb, 76.30.-v, 75.10.Jm

*Introduction.*— Recently, low-dimensional spin systems have received a considerable amount of attention. This is particularly due to their relevance to the quantum criticality problem, which appears to be one of the central concepts in modern solid state physics. Quantum fluctuations, significantly enhanced in spin systems with reduced dimensionality, give rise to a variety of strongly correlated states and make low-dimensional magnets an ideal ground for testing various theoretical concepts. To comprehend the role of quantum fluctuations in strongly correlated electron and spin systems with reduced dimensionality, it is important to explore its phenomenology in simple and well-controlled model systems. In this context, understanding the nature of the ground state and excitations in quantum spin chains is an important challenge. An isotropic  $S = \frac{1}{2}$  Heisenberg antiferromagnetic (AF) chain with uniform nearest-neighbor exchange coupling represents one of the paradigm models of quantum magnetism. Its ground state is a spin singlet, and the dynamics are determined by a gapless two-particle continuum of spin- $\frac{1}{2}$  excitations, commonly referred to as spinons. A uniform external magnetic field causes a substantial rearrangement of the excitation spectrum, making the soft modes incommensurate [1, 2], although the spinon continuum remains gapless. Since the  $S = \frac{1}{2}$  AF chain is critical, even small perturbations can considerably change fundamental properties of the system. One of the most prominent examples is the  $S = \frac{1}{2}$  AF chain perturbed by an alternating  $g$ -tensor and/or the Dzyaloshinskii-Moriya (DM) interaction; this situation is realized experimentally in several spin chain systems [3, 4, 5, 6, 7]. In the presence of such interactions, application of a uniform external field  $H$  induces an effective transverse staggered field  $h \propto H$ , which leads to the opening of an energy gap  $\Delta \propto H^{2/3}$ . The gapped phase can be effectively described by the quantum sine-Gordon field theory [8, 10]. The excitation spectrum is represented by solitons, antisolitons, and multiple soliton-

antisoliton bound states called breathers. The availability of exact solutions for the sine-Gordon model allows very precise theoretical description of many observable properties and physical parameters of sine-Gordon magnets, including field dependence of excitation energies [8, 9, 10] and response functions [11, 12]. This makes such systems a particularly interesting target for experimentally probing elementary excitations. So far, a field-induced gap has been observed in several  $S = \frac{1}{2}$  AF chain materials [3, 4, 5, 6, 7, 13]. At the same time, experimental information on the magnetic field behavior of the spectrum is rather limited, and usually only the lowest one or two excitations can be identified. In the most detailed existing study [7], a soliton and two breather modes were observed in  $\text{CuCl}_2 \cdot 2(\text{dimethylsulfoxide})$  (CDC) using inelastic neutron scattering. However, significant interchain interactions present in CDC lead to a pronounced deviation from the sine-Gordon model predictions. In ESR studies of copper benzoate [4, 13], several modes were observed but only the lowest one was identified.

In this Letter we report a detailed study of the elementary excitation spectrum in copper pyrimidine dinitrate (hereafter Cu-PM), which has been recently identified as a  $S = \frac{1}{2}$  AF chain with a field-induced spin gap [5], and is probably the best realization of the quantum sine-Gordon spin chain model known to date. Its intrachain exchange constant  $J = 36$  K [5, 14] is a factor of four larger than that in CDC [15] and about two times larger compared to copper benzoate [3]. It makes Cu-PM an excellent object for the experimental study of  $S = \frac{1}{2}$  AF chains in the low-temperature “nonperturbative” regime [16], where the temperature  $T$  is small compared to the energy gap  $\Delta$ . By employing high-resolution tunable-frequency submillimeter wave electron spin resonance (ESR) spectroscopy, *ten* different ESR modes were resolved and their behavior in a wide range of magnetic fields up to  $g\mu_B H \sim J$  was studied. By comparing the experimental data with

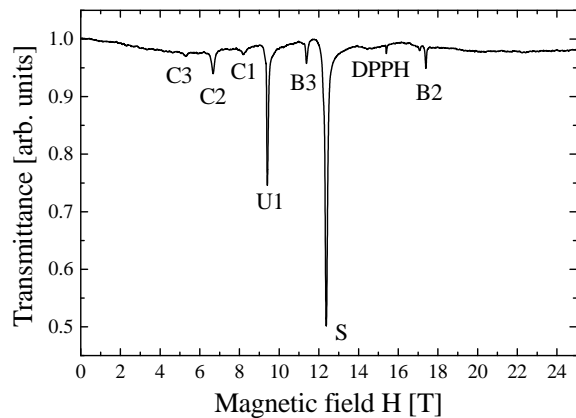


FIG. 1: The ESR transmission spectra in Cu-PM, taken in the Faraday configuration at a frequency of 429.3 GHz at  $T = 1.6$  K (for explanations see the text). DPPH was used as a marker.

the calculations based on the quantum sine-Gordon field theory, we were able to identify signatures of the *three lowest breathers* and of a *soliton*.

*Experimental.*— Cu-PM,  $[\text{PM-Cu}(\text{NO}_3)_2(\text{H}_2\text{O})_2]_n$  (PM = pyrimidine) crystallizes in a monoclinic structure belonging to space group  $C2/c$  with four formula units per unit cell [5]. The lattice constants obtained from the single-crystal X-ray diffraction are  $a = 12.404$  Å,  $b = 11.511$  Å,  $c = 7.518$  Å,  $\beta = 115.0^\circ$ . The Cu ions form chains (with a distance  $d = 5.71$  Å between neighboring  $\text{Cu}^{2+}$  ions at 10 K) running parallel to the short  $ac$  diagonal. The Cu ions are linked by the N-C-N moieties of pyrimidine, which constitute the intrachain magnetic exchange pathway. The interchain Cu-Cu distance is 6.84 Å. The Cu coordination is a distorted octahedron, built from an almost square N-O-N-O equatorial plane and two oxygens in the axial positions. In this approximately tetragonal local symmetry, the local principal axis of each octahedron is tilted from the  $ac$  plane by  $\pm 29.4^\circ$ . Since this axis almost coincides with the principal axis of the  $g$ -tensor, the  $g$ -tensors for neighboring Cu ions are staggered. The exchange constant  $J = 36 \pm 0.5$  K was extracted from the single-crystal susceptibility [5] and confirmed by magnetization measurements [14].

The excitation spectrum was studied using a high-field submillimeter wave ESR spectrometer [17]. Backward Wave Oscillators were employed as tunable sources of radiation, quasi-continuously covering the frequency range of 150 to 700 GHz. These radiation sources in combination with the highly-homogeneous magnetic field provided by a 25 T Bitter-type resistive magnet make the facility a powerful tool for studying magnetic excitation spectra in highly correlated spin systems. The magnetic field was applied along the  $c''$  direction, which is characterized by the maximal value of the staggered magnetization for Cu-PM [5, 18]. Our measurements at room tem-

perature yield  $g = 2.24 \pm 0.02$  as the effective  $g$ -factor for the field applied along the  $c''$  direction, which is consistent with the data of Ref. [5]. High-quality single-crystals of Cu-PM were probed using both Faraday and Voigt geometry sampleholders. We found that the spectra obtained in the Faraday and Voigt configurations exhibit a pronounced similarity (possible reasons for that will be discussed below).

Several resonance modes with different intensities were observed in experiments. A typical ESR transmittance spectrum obtained at a frequency of 429.3 GHz and at temperature  $T = 1.6$  K is shown in Fig. 1. Within the experimental accuracy, the absorptions can be nicely fit using the Lorentzian formula for the line shape. The complete frequency-field diagram of magnetic excitations, collected at  $T = 1.6$  K, is presented in Fig. 2. Absorptions denoted as B1, S and U1 have maximal intensity, while the rest of excitations are about one order of magnitude weaker. It is worthwhile to mention here that the low-temperature behavior of their integrated intensity, carefully checked at several temperatures down to 1.6 K, strongly suggests the ground state nature of the observed excitations (details of the temperature evolution of the excitation spectrum in Cu-PM will be reported elsewhere [19]).

*Discussion.*— The experimental frequency-field diagram has been analyzed in the framework of the quantum sine-Gordon field theory approach [8, 10]. We used the following expression [10] for the soliton gap  $\Delta_s$  which is valid for a wide range of fields up to  $g\mu_B H \sim J$ :

$$\Delta_s = J \frac{2\Gamma(\frac{\xi}{2})v_F}{\sqrt{\pi}\Gamma(\frac{1+\xi}{2})} \left[ \frac{g\mu_B H}{Jv_F} \frac{\pi\Gamma(\frac{1}{1+\xi})cA_x}{2\Gamma(\frac{\xi}{1+\xi})} \right]^{\frac{1+\xi}{2}}. \quad (1)$$

Here  $c$  is the proportionality coefficient connecting the uniform applied field  $H$  and the effective staggered field  $h = cH$ , the parameter  $\xi = (2/(\pi R^2) - 1)^{-1}$ , where  $R$  is the so-called compactification radius, and  $v_F$  has the meaning of the Fermi velocity. Both  $R$  and  $v_F$  are known exactly as functions of  $\tilde{H} = g\mu_B H/J$  from the solutions of the Bethe ansatz equations [10]. The amplitude  $A_x$ , which is also a function of  $\tilde{H}$ , was recently computed numerically [12]. At a given field  $H$ , there are  $N = [1/\xi]$  breather branches  $B_n$  with  $n = 1, \dots, N$ . The breather gaps  $\Delta_n$  are given by the formula

$$\Delta_n = 2\Delta_s \sin(n\pi\xi/2). \quad (2)$$

At  $H=0$  the first breather  $B_1$  is degenerate with the soliton-antisoliton doublet  $S, \bar{S}$ . At finite  $H$  this degeneracy is lifted, so that  $B_1$  becomes the lowest excitation and gives the strongest contribution into the magnitude of the gap observed in specific heat experiments [5]. The sine-Gordon model predicts two more “heavy” breathers  $B_2, B_3$  to exist in the relevant frequency-field range.

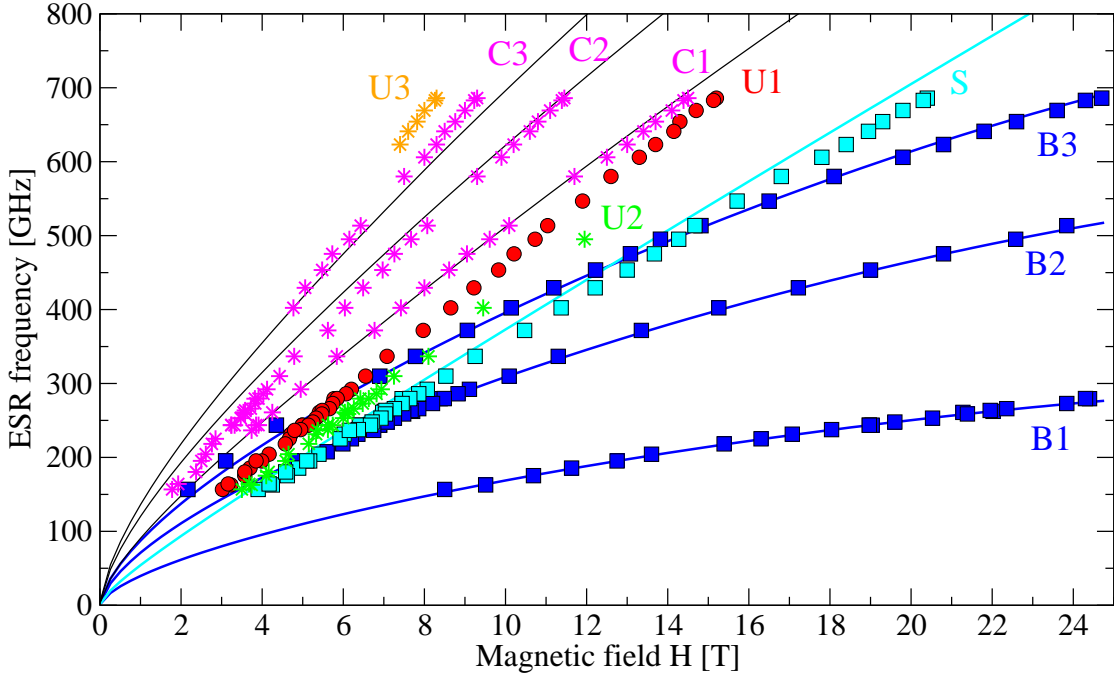


FIG. 2: The frequency-field dependence of the ESR modes in Cu-PM at  $T = 1.6$  K. Symbols denote the experimental results, and lines correspond to contributions from specific excitations as predicted by the sine-Gordon theory (see the text).

ESR probes the dynamical susceptibility  $\chi(q, \omega)$  at the momentum  $q = 0$ . However, in the present case the alternation of the  $g$ -tensor and DM interaction leads to a mixing of  $q = 0$  and  $q = \pi$  components. Moreover, due to the effective redefinition of spin operators which is performed to eliminate the DM interaction [10], and due to the fact that the Dzyaloshinskii vector is directed at an angle of about  $58^\circ$  with respect to the magnetic field [5], the physical susceptibility  $\chi_{\text{phys}}$  is generally a mixture of effective longitudinal and transverse susceptibilities  $\chi_{sG}$  calculated within the sine-Gordon model. For instance, the physical transverse susceptibility  $\chi_{\text{phys}}^\perp(0, \omega)$  is determined not only by  $\chi_{sG}^\perp(0, \omega)$ , but also gets a finite contribution from  $\chi_{sG}^\perp(\pi, \omega)$  and  $\chi_{sG}^\parallel(\pi, \omega)$ ; similarly, the longitudinal component  $\chi_{\text{phys}}^{zz}(0, \omega)$  contains a small admixture of  $\chi_{sG}^{xx}(0, \omega)$  and  $\chi_{sG}^{yy}(\pi, \omega)$ . For the analysis of inelastic neutron experiments probing  $q \approx \pi$ , this mixing could be safely neglected [10] since typically  $\chi(0, \omega) \ll \chi(\pi, \omega)$ , but it becomes important for the interpretation of ESR spectra, where even a small admixture of  $\chi(\pi, \omega)$  can have intensity comparable to that of  $\chi(0, \omega)$ . As a result, one should be able to observe contributions from  $\chi_{sG}^\perp$  as well as from  $\chi_{sG}^\parallel$  both in the Faraday and Voigt geometries.

The energy structure of elementary excitations of the sine-Gordon model contributing to the low-energy spin dynamics is sketched in Fig. 3. Single-particle contributions to the longitudinal susceptibility  $\chi_{sG}^\parallel$  are deter-

mined by solitons concentrated around incommensurate wave vectors  $q = \pi \pm k_0$  and by breathers concentrated around  $q = 0$ . Here the incommensurate shift  $k_0 = 2\pi m$  is determined by the total magnetization per spin  $m$ , exactly known as a function of the field; for small  $H$  one has  $Jv_F k_0 \approx g\mu_B H$ . In the transverse susceptibility  $\chi_{sG}^\perp$  the dominating contribution comes from breathers at  $q = \pi$  and solitons at  $q = \pm k_0$ . Thus, in an ESR experiment there should be several breather resonances at the energies  $\Delta_n$  as well as a single soliton resonance at

$$E_s \simeq \sqrt{\Delta_s^2 + (Jv_F k_0)^2}. \quad (3)$$

This exhausts the set of possible single-particle resonances (see Fig. 3); apart from them, there are various multiparticle continua contributing to the spectrum.

It is important to mention that in Eqs. (1)-(3) the only free fitting parameter is the coefficient  $c$ . Setting  $c = 0.08 \pm 0.002$ , we were able to achieve an excellent fit to the lowest observed mode B1, which is described by the first breather gap  $\Delta_1$ . Using this value of  $c$ , we calculated energies of other modes predicted by the sine-Gordon model, and obtained a reasonably good fit to the entire set of the experimental data. On the basis of the fit, we identify the observed resonances as follows: the modes B1, B2 and B3 correspond to the first three breather resonances at  $\Delta_1$ ,  $\Delta_2$  and  $\Delta_3$ , respectively (blue lines in Fig. 2). The mode S is well fitted by the soliton resonance at  $E_s$  (the cyan line in Fig. 2). This interpretation is supported by the analysis of the temperature dependence of

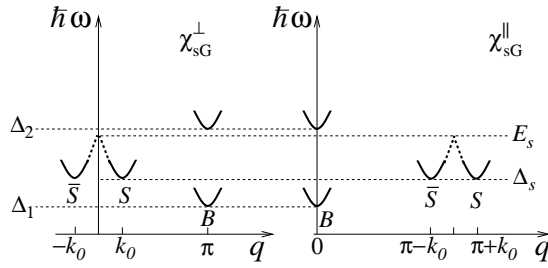


FIG. 3: A schematic view of low-energy excitations contributing to the transverse (left panel) and longitudinal (right panel) dynamic susceptibilities;  $\bar{S}$  ( $S$ ) denotes (anti)solitons and  $B$  labels breathers.

the ESR spectra, which shows that the  $S$  mode continuously transforms into the  $\omega = gH$  resonance when the temperature increases, in agreement with the theory [16]. The overall agreement between the sine-Gordon theory predictions and the experimentally obtained frequency-field dependence for those four single-particle resonances is very good. Note however that our value  $c = 0.08$  differs from the result  $c = 0.11$  obtained recently [14] from the analysis of magnetization curves of Cu-PM; the origin of this discrepancy is not clear at present.

The identification of the other six high-frequency ESR modes is more difficult since the theory does not predict any single-particle contributions in the relevant frequency region. One may nevertheless speculate that modes C1-C3 lie very close to the edges of the soliton-breather continua  $SB_1$ ,  $SB_2$  and  $SB_3$ , respectively, denoted by black lines in Fig. 2. The edges of the  $B_1B_1$  and  $S\bar{S}$  continua were not observed, presumably because they are close to the lines  $B1$  and  $B2$  and are masked by the corresponding quasiparticle contributions. For the remaining three modes U1-U3 we were not able to find any appropriate explanation on the basis of the sine-Gordon model, although we checked all possible two- and three-particle continua. This is especially puzzling in case of the U1 mode, which is one of the most intensive excitations (see Fig. 1). We hope that our observations will stimulate further theoretical work in this direction.

In summary, we have presented a detailed frequency-field diagram of spin excitations in Cu-PM, a material containing  $S = \frac{1}{2}$  AF chains with alternating  $g$ -tensor and DM interaction and exhibiting a field-induced gap. The use of high-resolution submillimeter wave ESR spectroscopy made possible obtaining a very precise information on the magnetic excitation spectrum. The field-induced gap was observed *directly*, and its high-field behavior was studied. *Ten* ESR modes were resolved and their behavior in a broad field range up to  $g\mu_B H \sim J$  was studied. By comparing the entire set of data with the theoretical predictions, we have provided experimental evidence for a number of excitations of the sine-Gordon theory, including *solitons* and the *three* lowest members

of the breather hierarchy. At the same time, we observed at least one strong high-frequency resonance mode which does not fit into the sine-Gordon model description. Our results can be relevant to understanding the quantum spin dynamics in copper benzoate and other  $S = \frac{1}{2}$  Heisenberg antiferromagnetic chain systems.

*Acknowledgments.*— We express our special thanks to F. H. L. Essler and C. Broholm for critical reading of the manuscript and valuable comments. We are also grateful to A. Honecker and A. U. B. Wolter for fruitful discussions. Experiments performed at NHMFL were supported by the NSF through Cooperative Grant DMR-9016241. A.K. was supported by Grant I/75895 from Volkswagen-Stiftung.

- 
- [1] G. Müller, H. Thomas, H. Beck and J. C. Bonner, Phys. Rev. B **24**, 1429 (1981).
  - [2] M. B. Stone, D. H. Reich, C. Broholm, K. Lefmann, C. Rischel, C. P. Landee, and M. M. Turnbull, Phys. Rev. Lett. **91**, 037205 (2003).
  - [3] D. C. Dender, P. R. Hammar, D. H. Reich, C. Broholm and G. Aeppli, Phys. Rev. Lett. **79**, 1750 (1997).
  - [4] T. Asano, H. Nojiri, Y. Inagaki, J. P. Boucher, T. Sakon, Y. Ajiro and M. Motokawa, Phys. Rev. Lett. **84**, 5880 (2000).
  - [5] R. Feyerherm, S. Abens, D. Günther, T. Ishida, M. Meißner, M. Meschke, T. Nogami and M. Steiner, J. Phys.: Condens. Matter **12**, 8495 (2000).
  - [6] M. Kohgi, K. Iwasa, J.M. Mignot, B. Fak, P. Gegenwart, M. Lang, A. Ochiai, H. Aoki and T. Suzuki, Phys. Rev. Lett. **86**, 2439 (2001).
  - [7] M. Kenzelmann, Y. Chen, C. Broholm, D.H. Reich and Y. Qiu, preprint cond-mat/0305476.
  - [8] M. Oshikawa and I. Affleck, Phys. Rev. Lett. **79**, 2883 (1997).
  - [9] F. H. L. Essler, Phys. Rev. B **59**, 14376 (1999).
  - [10] I. Affleck and M. Oshikawa, Phys. Rev. B **60**, 1038 (1999); *ibid.* **62**, 9200 (2000).
  - [11] F. H. L. Essler and A. M. Tsvelik, Phys. Rev. B **57**, 10592 (1998).
  - [12] F. H. L. Essler, A. Furusaki, and T. Hikihara, Phys. Rev. B **68**, 064410 (2003).
  - [13] T. Asano, H. Nojiri, Y. Inagaki, T. Sakon, J.P. Boucher, Y. Ajiro and M. Motokawa, Physica B **329-333**, 1213 (2003).
  - [14] A. U. B. Wolter, H. Rakoto, M. Costes, A. Honecker, W. Brenig, A. Klümper, H.-H. Klauss, F.J. Litterst, R. Feyerherm, D. Jérôme, and S. Süllo, Phys. Rev. B **68**, 220406 (2003).
  - [15] C. P. Landee, A. C. Lamas, R. E. Greeney and K. G. Bücher, Phys. Rev. B **35**, 228 (1987).
  - [16] M. Oshikawa and I. Affleck, Phys. Rev. Lett. **82**, 5136 (1999); Phys. Rev. B **65**, 134410 (2002).
  - [17] S. A. Zvyagin *et al.*, unpublished.
  - [18] T. Asano, D. Nomura, Y. Inagaki, Y. Ajiro, H. Nojiri, Y. Narumi, K. Kindo, T. Ishida, and T. Nogami, Physica B **329**, 1006 (2003).
  - [19] S. A. Zvyagin *et al.*, unpublished.